Thin Film Growth Related Adsorption Study of Al and O Ions on an α-Al_2O_3 Surface

Johanna Rosén,*,† Jochen M. Schneider,† and Karin Larsson‡

Materials Chemistry, RWTH-Aachen, D-52056 Aachen, Germany, and Department of Materials Chemistry, The Ångström Laboratory, Uppsala University, Box 538, 751 21 Uppsala, Sweden

Received: April 23, 2004; In Final Form: September 17, 2004

The surface reactivity of α-Al_2O_3 (0001) has been investigated theoretically using density functional theory. The adsorption process of Al^+, Al^{2+}, Al^{3+}, and O^+ were studied to identify possible preferential adsorption sites during thin film growth. Differences in near surface atomic displacements (e.g., adsorption-induced surface reconstructions), energies, and bonding character have been evaluated. The adsorption energies for the metallic ions showed a strong dependence on both initial charge and adsorption site. The O^+ ions showed no site dependence, but adsorption energies similar to those calculated for Al^+. The results indicate that the adsorption of O^+ and Al^{3+} may favor the formation of an amorphous structure, which is consistent with experimental observations. The results are of fundamental importance for the understanding of thin film microstructure evolution.

I. Introduction

At standard conditions, α-Al_2O_3 is the only thermodynamically stable phase of aluminum oxide and of large interest for both science and technology. The applications range from thin dielectric in microelectronics and catalytic support[1] to corrosion and wear protection[2] in mechanical systems. α-Al_2O_3 has served as a prototype for understanding metal oxides through numerous experimental and theoretical investigations. Some of these investigations suggest that the relaxed crystal structure with a single terminating Al layer (0001) result in the most stable *clean* surface, shown theoretically in, for example, refs 3−6, and also experimentally in refs 7 and 8. However, the termination is still a matter of debate; Calculations of Barytrev et al. suggest that oxygen termination is stable by exposure at an oxygen pressure of ∼100 kPa.[9] Renaud reported O-terminated structures that were prepared by heating in an oxygen rich atmospheres,[10] and Jaeger[11] suggested the same termination on the basis of experimental investigations on ultrathin films of alumina. Toofan and Watson found both O and Al terminated domains in a 2:1 ratio[12] using low energy electron diffraction (LEED) analysis, a mixture that was also observed by Ahn.[13] The discrepancy between different theoretical predictions and experimental results may be explained by the presence of hydrogen. The O-terminated surface is expected to be unstable due to the nonzero dipole moment resulting from the stacking sequence, O−Al−Al, of the crystal. However, adding one hydrogen per unit cell drastically lowers the free energy[14] and therefore stabilizes the O-terminated surface. Calculations show that a hydrated (0001) surface is oxygen terminated.[15,16] Hydrogen stemming from the residual gas may be present during thin film growth,[17] and detailed experimental investigations have detected H chemisorbed to the surface,[13,16,18] as well as H that was incorporated during thin film growth.[19,20] Therefore, an O-terminated α-Al_2O_3 surface has been chosen for the present adsorption investigation.

Surface reactivity and adsorption studies have earlier been reported for α-Al_2O_3 (0001). The exposure of the Al terminated surface to various metals were investigated in refs 21−27. For O-terminated surfaces, Kruse et al. reported Nb interaction with the oxide,[27] Bogicevic et al. studied metal adsorption (1/3−4 ML) on ultrathin films,[28] and Lodziana calculated the interaction of Cu and Pd (1 ML) with the surface.[22] These latter investigations show that, in comparison to Al terminated surfaces, the interaction with O-terminated surfaces is stronger,[22] more ionic (especially at low coverages),[22,28] and there are also indications of preferred adsorption sites.[28]

No systematic adsorption study of Al^+, Al^{2+}, Al^{3+}, and O^+ on an O-terminated α-Al_2O_3 (0001) surface is available in the literature. Here, density functional theory (DFT) calculations have been used for this purpose. The ions chosen have been observed in plasma chemistry measurements of an Al arc plasma in an oxygen environment, in the presence of magnetic fields[29] as well as without magnetic fields.[17] Furthermore, an O-terminated surface can be motivated by both the presence of oxygen *and* the additional detection of hydrogen in the plasma.[17,29] The results presented are of fundamental importance for the understanding of the evolution of thin film microstructure.

II. Method

Three differently located adsorption sites were chosen on the O-terminated α-Al_2O_3 (0001) surface; see Figure 1. The sites were A, above an Al atom in the third atomic layer, B, above an O atom in the fourth layer, and C, above an Al atom in the second layer. Site A corresponds to the bulk position of an Al ion, whereas B and C interrupt the crystalline sequence of positions. The adsorbates were initially positioned at these sites (approximately 1 Å over the surface), and the subsequent geometry optimization resulted in the structure for which the total energy was calculated. The adsorption energies, E_{ads}, of the different ions were calculated using

$$E_{ads} = E_{a+s} - (E_a + E_s) \quad (1)$$

where E_a is the energy of the free ion (with charge $+q$), E_s is the total energy of the relaxed surface without adsorbate (with

† RWTH-Aachen.
‡ Uppsala University.

10.1021/jp048225+ CCC: $27.50
Published on Web 12/09/2004

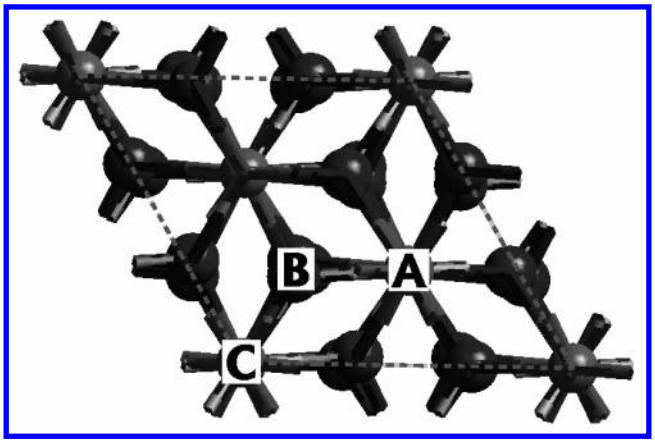

Figure 1. Unit cell (top view) of the α-Al_2O_3 (0001) surface with investigated adsorption sites A, B, and C. The cell size used in the calculations is 2 × 2 unit cells laterally.

charge $-q$) and E_{a+s} is the total energy of the relaxed surface with adsorbate (total system neutral). The ionic species used as adsorbates (plausible film forming species) were Al^+, Al^{2+}, Al^{3+}, and O^+, as detected by charge to mass spectrometry.[17,29]

The geometrical structure and total energies of the reactants and products in eq 1 were obtained by using ab initio quantum mechanical calculations, within the framework of density functional theory (DFT) under periodic boundary conditions. The program package CASTEP from Accelrys Inc. was used for these calculations.[30] A supercell approach, resulting in a two-dimensional slab, did then represent the α-Al_2O_3 (0001) surface. For more details of the model size, see section III. Only the valence electrons of the system were explicitly treated, and these orbitals were represented by a plane-wave expansion including all plane waves up to the chosen cutoff energy of 260 eV. The *k*-points (1) used for the plane-waves were generated according to Monkhorst−Pack,[31] which produces a uniform mesh of points in reciprocal space. The density mixing scheme was utilized for electronic minimization, and the electron−ion interaction was described by an ultrasoft pseudopotential in the Kleinman−Bylander form.[32]

DFT methods use various approximations to describe the exchange and correlation interactions between the electrons. The commonly used local density approximation (LDA/LSDA) results in rather accurately described local properties such as bond lengths. However, this method tends to overestimate the bond energies. The more accurate generalized gradient approximation (GGA/GGS) methods involve improved treatment of inhomogeneities in the electron density, resulting in improved results of the global changes in energy (e.g., bond energy).[33,34] In the present study, the LDA/LSDA method was used for the geometry optimization, whereas the generalized gradient approximation method (GGA/GGS) was used for the subsequent single-point-energy calculations. The adsorption process of different ionic species were thoroughly investigated by calculating not only the adsorption energy but also atomic charges, bond populations, bond lengths, and adsorption-induced changes in surface structural geometries.

III. Test Calculations

As described above, the α-Al_2O_3 (0001) surface is being modeled in a supercell approach, which is repeated periodically in three dimensions and, thereby, forms an infinite slab. One of the requirements is therefore that the thickness of the slab, as well as the vacuum layer between the slabs, is large enough to facilitate a negligible interaction between the individual cell surfaces. Furthermore, the width of the cell is of importance to avoid interaction between adsorbates in adjacent cells.

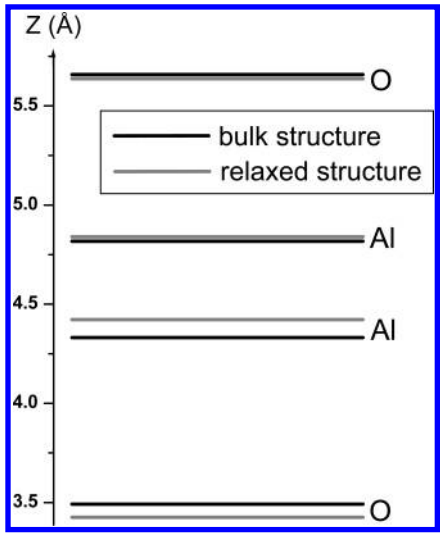

Figure 2. Schematic side view of the topmost layers in the super cell, before and after surface relaxation.

The test calculations involved calculations of the adsorption energy of Al^+ in its bulk position on an α-Al_2O_3 (0001) surface, and the cell was enlarged until convergence in adsorption energy (<3% difference) was obtained. The size of the slab in the *x*, *y*, and *z* directions, the vacuum layer, and the number of movable atoms were then varied. The resulting O-terminated slab contains three layers of oxygen (O−Al−Al−O−Al−Al−O−Al−Al), which is a thickness reported to be well suited for surface energy studies.[35,36] The hexagonal supercell size is 9.52, 9.52, and 12.99 Å (with a vacuum depth of 7.4 Å), which is consistent with literature to be large enough to ignore mutual influence of the surfaces.[7,35,36] The lowest four atomic layers are fixed during geometry optimization to simulate bulk conditions, which did not significantly influence (<3% deviation) the resulting calculated adsorption energies. Additionally, different approximations were tested; number of *k*-points, whether to use gradient corrections (GGA vs LDA) or explicitly take spin into account (LDA vs LSDA, GGA vs GGS).

A schematic side view of the topmost layers in the supercell can be seen in Figure 2, showing the calculated surface relaxation in *z* direction. As can be seen, there is only a minor relaxation of the terminating O layer, which is consistent with literature.[9,15,22] The changes in the first three interplanar spacings are −5.1, −14, and +18%, a trend in good agreement with refs 15 and 22. The shift of the two aluminum layers toward the surface has also been observed in MD studies of the surface relaxation, explained to be due to the field of unbalanced electric dipoles.[5] In addition, a minor atomic displacement (surface reconstruction) in the horizontal plane was observed.

IV. Results and Discussion

Plasma production by cathodic arc results in ions that move with a directed velocity toward the substrate surface to eventually form a thin film. The surface reactivity will most probably affect the incorporation site and may therefore influence the resulting structure evolution. The effect of surface site and charge of the metal adsorbate on the adsorption energy, as well as the nature of the adsorbate−surface bonding situation, have been investigated. The adsorption of O^+, the most abundant nonmetal ion detected in an Al arc plasma in an oxygen environment has also been included.[29]

TABLE 1: Adsorption Energy (E_{Ads}) and Final Charge (C_f) of the Al Ions at the Adsorption Sites

	Al^+		Al^{2+}		Al^{3+}	
	E_{ads} (eV)	C_f	E_{ads} (eV)	C_f	E_{ads} (eV)	C_f
A	−20.98	1.96	−36.70	1.95	−(x+4.67)	1.96
B	−19.19	1.95	−34.71	1.93	−(x+4.21)	1.90
C	−15.42	1.89	−30.70	1.88	−(x)	1.88

A. Metal Adsorption. *1. Charge Dependence.* The influence of the charge of the adsorbate (also referred to as charge state) on the adsorption behavior, was studied by comparing adsorption of different ions at identical surface sites. As can be seen in Table 1, the initial charge of all Al ions was found to clearly affect the magnitude of the adsorption energy, E_{ads}, at all surface sites studied (A, B, or C). Because ultrasoft pseudopotential functions were used in the calculations, adsorption energies could only be calculated for Al^+ and Al^{2+} ions. E_{ads} was, for all surface sites, found to be strongly exothermic, and was for Al^{2+} approximately 16 eV larger than for Al^+. It is reasonable to assume that the main contribution to this difference is the *initial potential energy difference*. Additionally, as the free ion moves toward the surface, several subprocesses will occur (e.g., subsequent charge transfer and relaxation) that generally result in a decrease in total energy to an equilibrium value. Turning to Table 1, it can be seen that the final charges of the adsorbates (at identical adsorption sites) are similar. From this one can conclude that the charge transfer between the adsorbate and the surface is strongly dependent on the charge of the adsorbate. The first and second ionization energies of Al are 6 and 18.8 eV, respectively.[37] Furthermore, one additional charge added to the surface prior to adsorption results in a calculated increase in total energy of 2.9 eV. Close to one electron is transferred to the surface during Al^+ adsorption, whereby an adsorption energy can be estimated from the difference between the ionization energy of Al^+, and the energy increase associated with the additional charging of the surface, (18.8−2.9) 15.9 eV. The calculated difference in adsorption energy between Al^+ and Al^{2+} is 15.3 to 15.7 eV, which in Figure 3 can be compared to the inserted bars of 15.9 eV.

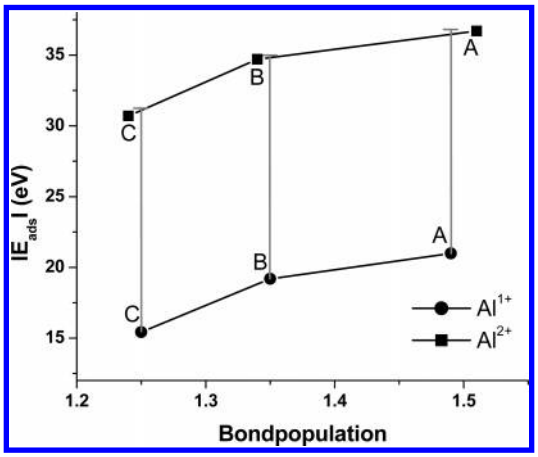

Figure 3. Adsorption energy ($|E_{ads}|$) versus bond population for Al^+ and Al^{2+} ions adsorbed on the surface sites A, B, and C.

Other contributions to the adsorption energy can be discussed in terms of surface reconstructions, and adsorbate−surface bonding. As can be seen in Table 2, the calculations for both Al^+ and Al^{2+} resulted in the formation of three Al−O bonds between adsorbate and surface (for all of the three sites studied). The bond population is correlated to the electron density in the bonding region between two atoms, indicating the contribution of covalent bonding to the overall bonding character. No significant differences in bond lengths and bond populations for the different ions at an identical site can be detected. In addition, the large similarity in final charge and bond lengths for the adsorbates (at identical surface sites; see Table 1) indicate no significant difference in the ionic contribution to the overall bonding character either. These observations underline the suggested role of the difference in initial potential energy for the adsorption energy differences discussed.

TABLE 2: Bond Lengths and Bond Populations between the Al Adsorbates and the Adsorbate-Binding Surface Atoms (Denoted O_{nr})

		Al^+		Al^{2+}		Al^{3+}	
	atom	pop.	bond length (Å)	pop.	bond length (Å)	pop.	bond length (Å)
A	O_{36}	0.50	1.67	0.50	1.67	0.50	1.67
	O_{30}	0.50	1.67	0.50	1.67	0.50	1.67
	O_{26}	0.49	1.68	0.51	1.67	0.50	1.67
B	O_{28}	0.47	1.63	0.46	1.64	0.44	1.68
	O_{32}	0.47	1.65	0.47	1.67	0.45	1.70
	O_{36}	0.41	1.73	0.41	1.75	0.19	2.24
	O_{34}					0.47	1.72
C	O_{25}	0.42	1.72	0.42	1.72	0.42	1.72
	O_{36}	0.42	1.72	0.41	1.72	0.41	1.72
	O_{32}	0.41	1.72	0.41	1.72	0.42	1.72

TABLE 3: Total Energy (E_t) of the Resulting Configurations (Surface + Adsorbate) Relative to the Structure of Lowest Energy (Al^{2+} Adsorbed on Site A)

	Al^+ E_t (eV)	Al^{2+} E_t (eV)	Al^{3+} E_t (eV)
A	0.19	0	0.11
B	1.92	1.99	0.57
C	5.69	6.0	4.78

The total energy of the final structure (surface + adsorbate) was found to be independent of the initial charge of the adsorbate, with the exception of Al^{3+} adsorbing on the non-equilibrium sites B and C, respectively (see Table 3). This may be due to the increased number of nearest neighbors (around B and C) accompanying the charge transfer between adsorbate and surface, with resulting larger atomic displacements detected (more accentuated for site B). This is indicated in Table 2 (site B), where a clear difference in bond length and population for Al^{3+} and the other two adsorbates can be seen.

2. Site Dependence. Significant energy differences are found when adsorption of one specific ion at different adsorption sites is compared; see Table 1. When the site dependence for Al^+ is studied, the adsorption energy is calculated to −21.0, −19.2, and −15.4 eV for sites A (equilibrium site, above Al), B (nonequilibrium site, above O), and C (nonequilibrium site, above Al), respectively. The ions Al^{2+} and Al^{3+} show the same trend. This may be understood by analyzing the bonding situation between the adsorbate and its closest neighbors. It is well-known that the overall bond strength is sensitive to covalent, ionic, and metallic contributions. Here we investigate the site dependence of (a) the bond population and (b) the final charge state of the adsorbate, as a measure for the covalent and ionic contribution to the overall bond strength, respectively. It has earlier been shown that the magnitude of the bond populations correlates with the bond strength in various bulk crystals (including oxides).[38] The bond populations given in Table 2 show a decrease in magnitude in going from site A to site C (via site B). The adsorption energies for Al^+ and Al^{2+} versus the sum of the populations in the bonds between the adsorbate and its nearest neighbors is plotted in Figure 3. As

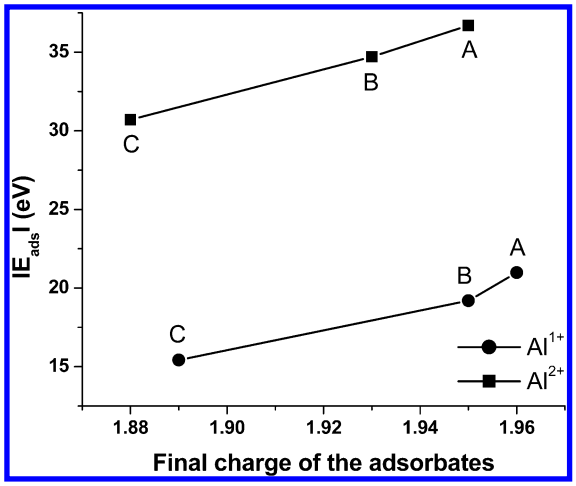

Figure 4. Adsorption energy ($|E_{ads}|$) versus final adsorbate charges for Al^+ and Al^{2+} ions adsorbed on the surface sites A, B, and C.

expected, an increase in bond population corresponds to an increase in adsorption energy, $|E_{ads}|$. The same trend is detected for the relative energies of Al^{3+}, though not as pronounced.

The ionic contribution to the overall bond strength is indicated in Table 1. In addition to the bond lengths, a comparison between the different relative ionic (and covalent) bond strengths can be made by looking at the final charge of the adsorbates. Moreover, the correlation between the adsorption energy for Al^+ and Al^{2+}, and the final charge of the adsorbates is shown in Figure 4. The lattice site A (with the largest adsorption energies) does correspond to the highest final adsorbate charges. Site C (with the smallest adsorption energies) has the lowest charges, and the result for site B is between A and C. When the results presented in Figure 4 and Table 2 are compared, a correspondence between an increased bond length, a decreased charge, and a decrease in ionic bond strength can hence be found in going from surface site A to C. The ordering of the surface adsorption sites on an adsorption energy scale may therefore be explained by an indicated change in bond strength for *both* the ionic and covalent parts. It should furthermore be noted that the ionic interaction is stronger at the surface as compared to in the bulk. This is evident from the charges of the adsorbates being close to 1.9 (Table 1) and the charges of Al in the middle of the slab being close to 1.7.

A comparison between the adsorption energy of different α-Al_2O_3 (0001) sites could possibly give information about preferred surface sites during thin film growth and consequently a clue to evolving crystal structures. All ions show strong exothermic reactions when adsorbed to different surface sites. Site A corresponds to a bulk equilibrium position of an Al ion and results in the highest adsorption energies (absolute values) of the three sites studied. Site B, though not a bulk position, results in a lower adsorption energy for the Al^+ and Al^{2+}ions, but for Al^{3+} adsorption site B shows a value (difference of 0.46 eV) similar to that for site A (Table 1). This similarity between A and B surface sites could indicate that, in the presence of Al^{3+} ions, it is likely that an amorphous material will evolve during film growth because the crystal bulk sites are then not energetically preferred.

The difference in magnitude of the adsorption energy indicates that there are barriers for surface migration between the different sites; otherwise the geometry optimization of the structure would have resulted in the same final location for the adsorbates. The height of these barriers will also strongly affect the evolving surface structure and may result in the formation of an amorphous structure.

TABLE 4: Adsorption Energy (E_{sds}) and Final Charge (C_f) of the O^+ Adsorbate, Together with the Bond Populations and Bond Lengths between the Adsorbate and the Adsorbate-Binding Surface Atoms (Denoted O_{nr})

	O^{1+}				
	E_{ads} (eV)	C_f	atom	pop.	bond length (Å)
A	−17.50	0.12	O_{30}	0.32	1.37
			O_{26}	0.24	1.47
			O_{36}	0.00	2.19
B	−16.93	0.11	O_{29}	0.30	1.39
			O_{37}	0.29	1.46
C	−17.20	−0.02	O_{36}	0.11	1.58
			O_{25}	0.09	1.59
			O_{32}	0.08	1.62

B. Nonmetal Adsorption (O^+). The oxygen ionic species O^+ is often the most abundant nonmetal ionic species in an Al/oxygen arc plasma.[29] By applying the same research strategy as for evaluating the strong surface site dependence of the Al ions, the adsorption energy of O^+ at the different sites (A, B, C) were found to show similar values (ranging from −16.9 to −17.5 eV); see Table 4. There is about one electron being transferred from the adsorbate to the surface. The initial charge of the adsorbate is +1, and the final ones are 0.12, 0.11, and −0.02 for sites A, B, and C, respectively. A comparison of the bond populations in Table 4 also shows lower total values for site C. One plausible contribution to these differences is the adsorption-induced surface geometry changes: Adsorption at *sites A and B* resulted in atomic displacements of the nearest neighbors in the top O layer (comparable to results of Al^+ and Al^{2+}). The second atomic layer (first Al layer) showed hardly any geometrical changes. The resulting adsorbate−surface distance were larger as compared to the Al adsorbates. The adsorption at *site C* resulted in a somewhat different final geometrical structure, with more changes in surface geometry than found at both sites A and B, and for the Al adsorbates at site C. Especially, the three closest binding atoms to the adsorbate showed an outward relaxation, though the resulting distance of the O adsorbate above the main part of the surface was comparable to the results of the Al adsorbates. The first Al layer was also influenced geometrically.

All three adsorption sites interrupt the crystalline atom sequence when O^+ is adsorbed, and all sites studied result in exothermic adsorption reactions. The adsorption of O^+ on an O-terminated α-Al_2O_3 (0001) surface with adsorption energies within 3.8 eV from those of Al^+, and at site C even 1.78 eV lower as compared to Al^+, may indicate amorphous growth for kinetically limited systems. Alumina synthesis by physical vapor deposition is known to result in the formation of an amorphous structure at substrate temperatures ≤250 °C.[39] It is therefore suggested that the here presented findings may at least in part serve as an explanation for the reported experiments.

V. Conclusion

The adsorption processes of Al^+, Al^{2+}, Al^{3+}, and O^+ on an O-terminated α-Al_2O_3 (0001) surface have here been investigated using quantum mechanical DFT methods under periodic boundary conditions. The goals were to identify plausible preferential adsorbate sites and to contribute toward an understanding of the microstructure evolution during growth of Al_2O_3 thin films. All adsorption reactions were found to be exothermic. Adsorption on the equilibrium (bulk) lattice position resulted in the most preferred adsorption situation. Numerically similar adsorption energies for Al^{3+} adsorbed on different surface sites

indicates that amorphous film growth may be likely to occur with Al^{3+} ions as film-forming material. The O^+ ions showed less dependence of adsorption energy on surface site, with energies similar to those calculated for Al^+ adsorption. These results may explain the experimentally observed formation of amorphous structures during kinetically limited alumina thin film growth.

Acknowledgment. This work was supported by the Swedish Research Council (VR). The computational results were obtained using the software programs from Accelrys. Inc. (first principle calculations were done with the CASTEP program within the Cerius2 program package). J.M.S. acknowledges sponsorship of the Alexander von Humboldt Foundation, the German Federal Ministry of Education and Research, and the Program for Investment in the Future.

References and Notes

(1) Henry, C. R. *Surf. Sci. Rep.* **1998**, *31*, 231.
(2) Dörre, E.; Hübner, H. *Alumina*; Springer-Verlag: Heidelberg, 1984.
(3) Mackrodt, W. C. *Phys. Chem. Miner.* **1988**, *15*, 228.
(4) Guo, J.; Ellis, D. E.; Lam, D. J. *Phys. Rev. B* **1992**, *45*, 13647.
(5) Blonski, S.; Garofalini, S. H. *Surf. Sci.* **1993**, *295*, 263.
(6) Puchin, V. E.; Gale, J. D.; Shluger, A. L.; Kotomin, E. A.; Günster, J.; Brause, M.; Kempter, V. *Surf. Sci.* **1997**, *370*, 190.
(7) Baxter, R.; Reinhardt, P.; López, N.; Illas, F. *Surf. Sci.* **2000**, *445*, 448.
(8) Walters, C. F.; McCarty, K. F.; Soares, E. A.; Van Hove, M. A. *Surf. Sci. Lett.* **2000**, *464*, L732.
(9) Batyrev, I.; Alavi, A.; Finnis, M. W. *Faraday Discuss.* **1999**, *114*, 33.
(10) Renaud, G. *Surf. Sci. Rep.* **1998**, *32*, 1.
(11) Jaeger, R. M.; Kuhlenbeck, H.; Freund, H.-J.; Wuttig, M.; Hoffmann, W.; Franchy, R.; Ibach, H. *Surf. Sci.* **1991**, *259*, 235.
(12) Toofan, J.; Watson, P. R. *Surf. Sci.* **1998**, *401*, 162.
(13) Ahn, J.; Rabalais, J. W. *Surf. Sci.* **1997**, *388*, 121.
(14) Wang, X.; Chaka, A.; Scheffler, M. *Phys. Rev. Lett.* **2000**, *84*, 3650.
(15) Tepesch, P. D.; Quong, A. A. *Phys. Status Solidi B* **2000**, *217*, 377.
(16) Eng, P. J.; Trainor, T. P.; Brown, G. E.; Waychunas, G. A.; Newville, M.; Sutton, S. R.; Rivers, M. L. *Science* **2000**, *288*, 1029.
(17) Schneider, J. M.; Anders, A.; Brown, I. G.; Hjörvarsson, B.; Hultman, L. *Appl. Phys. Lett.* **1999**, *75*, 612.
(18) Niu, C.; Sheperd, K.; Martini, D.; Kelber, J. A.; Jennison, D. R.; Bogicevic, A. *Surf. Sci.* **2000**, *465*, 163.
(19) Schneider, J. M.; Anders, A.; Hjörvarsson, B.; Petrov, I.; Macák, K.; Helmersson, U.; Sundgren, J.-E. *Appl. Phys. Lett.* **1999**, *74*, 200.
(20) Schneider, J. M.; Larsson, K.; Lu, J.; Olsson, E.; Hjörvarsson, B. *Appl. Phys. Lett.* **2002**, *80*, 1144.
(21) Gomes, J. R. B.; Illas, F.; Hernándes, N. C.; Sanz, J. F.; Wander, A.; Harrison, N. M. *J. Chem. Phys.* **2002**, *116*, 1684.
(22) Lodziana, Z.; Norskov, J. K. *J. Chem. Phys.* **2001**, *115*, 11261.
(23) Verdozzi, C.; Jennison, D. R.; Schultz, P. A.; Sears, M. P. *Phys. Rev. Lett.* **1999**, *82*, 799.
(24) Suzuki, T.; Hishita, S.; Oyoshi, K.; Souda, R. *Surf. Sci.* **1999**, *437*, 289.
(25) Ohuchi, F. S.; Kohyama, M. *J. Am. Ceram. Soc.* **1991**, *74*, 1163.
(26) Zhukovskii, Y. F.; Alfredsson, M.; Hermansson, K.; Heifets, E.; Kotomin, E. A. *Nucl. Instrum. Methods B* **1998**, *141*, 73.
(27) Kruse, C.; Finnis, M. W.; Lin, J. S.; Payne, M. C.; Milman, V. Y.; DeVita, A.; Gillan, M. J. *Philos. Mag. Lett.* **1996**, *73*, 377.
(28) Bogicevic, A.; Jennison, D. R. *Phys. Rev. Lett.* **1999**, *82*, 4050.
(29) Schneider, J. M.; Anders, A.; Yushkov, G. Y. *Appl. Phys. Lett.* **2001**, *78*, 150.
(30) Payne, M. C.; Teter, M. P.; Allan, D. C.; Arias, T. A.; Joannopoulus, J. D. *Rev. Mod. Phys.* **1992**, *64*, 1045.
(31) Monkhorst, H. J.; Pack, J. D. *Phys. Rev. B* **1976**, *13*, 5188.
(32) Kleinman, L.; Bylander, D. *Phys. Rev. Lett.* **1982**, *48*, 1425.
(33) Hammer, B.; Jacobsen, K. W.; Norskov, J. K. *Phys. Rev. Lett.* **1993**, *70*, 3971.
(34) Hu, P.; King, D. A.; Crampin, S.; Lee, M.-H.; Payne, M. C. *Chem. Phys. Lett.* **1994**, *230*, 501.
(35) Manassidis, I.; De Vita, A.; Gillan, M. J. *Surf. Sci. Lett.* **1993**, *285*, L517.
(36) Manassidis, I.; Gillan, M. J. *J. Am. Ceram. Soc.* **1994**, *77*, 335.
(37) *Handbook of Chemistry and Physics*, 72nd ed.; CRC Press: Boston, 1991.
(38) Segall, M. D.; Shah, R.; Pickard, C. J.; Payne, M. C. *Phys. Rev. B* **1996**, *54*, 16317.
(39) Schneider, J. M.; Sproul, W. D.; Chia, R. W. J.; Wong, M.-S.; Matthews, A. *Surf. Coat. Technol.* **1997**, *96*, 262.